Chapter 2

Glucocorticoid-induced attenuation of the inflammatory response in zebrafish

Antonia Chatzopoulou, Jeroen P.M. Heijmans, Herman P. Spaink, Annemarie H. Meijer, Marcel J.M. Schaaf

Abstract

Glucocorticoids are steroid hormones that are secreted by the adrenal gland upon stress. Their effects are mediated by the glucocorticoid receptor (GR) which acts as a transcription factor, regulating a wide plethora of genes. Since anti-inflammatory activity of glucocorticoids has been well established, they are widely used clinically to treat a variety of inflammatory and immune-related diseases. However, the exact specificity, mechanisms and level of regulation of different inflammatory pathways by GR signaling have not fully been elucidated. In the present study, a tail fin amputation assay was employed in 3-day-old zebrafish larvae in order to study the immunomodulatory effects of the synthetic glucocorticoid beclomethasone, using cell imaging as well as whole transriptome analysis. Our results show that amputation induced migration of both neutrophils and macrophages towards the wound site, and that beclomethasone treatment attenuated the migratory behavior of only neutrophils. In addition, the expression of many pro-inflammatory genes was induced upon amputation and this induction was suppressed by beclomethasone for virtually all induced genes. Apparently, glucocorticoid treatment has a very general dampening effect on the induction of gene expression upon amputation, without any specificity for particular pathways. These results show that the zebrafish larva model of tail fin amputation and beclomethasone treatment recapitulates the well known anti-inflammatory glucocorticoid effects, thus providing a reliable model system to further elucidate the molecular mechanisms of glucocorticoid signaling.

Introduction

Glucocorticoids (GCs) are potent anti-inflammatory agents that have been widely used clinically over the last 50 years for the treatment of many inflammatory and autoimmune diseases, graft rejection and malignancies of the immune system [1, 2]. The effects of GCs are mediated by the glucocorticoid receptor (GR), which is a nuclear receptor that is expressed almost ubiquitously in the human body and regulates a wide range of biological processes such as our metabolism, growth, reproduction, vascular tone, bone formation, immune response and brain function [3-8]. In its inactive state, the GR resides within the cytoplasm in a multiprotein complex containing chaperones and immunophilins [9]. Upon GC binding, it is released from this cytoplasmic complex and translocates to the nucleus, where it orchestrates gene expression via DNA-binding-dependent and -independent mechanisms. DNA-binding-dependent mechanisms involve GR occupancy of glucocorticoid response elements (GREs) and recruitment of transcriptional coregulators, resulting in a modulation of the transcription rate of target genes. Independent of DNA-binding, the GR can physically interact with other transcription factors via which it can either enhance the activity of these factors (e.g. in the case of STAT-5 activity on the IGF-1 promoter [6] or repress their activity (e.g. in the case of NF-κB or AP-1 activity on the promoter of a large number of cytokine genes) [3, 4, 6, 10-12]. The latter mode of action is termed *transrepression* and comprises one of the main mechanisms by which GCs exert their anti-inflammatory effects [3, 4, 9-13].

Many *in vitro* and *in vivo* studies have been performed to elucidate the cellular and molecular mechanisms underlying the effects of GR signaling on the immune system (for a review see Franchimont et al. [14]). From these studies it appeared that GCs suppress inflammation by downregulating the expression of a wide variety of pro-inflammatory

cytokines (e.g. IL1β, IL6, TNFα), chemokines (e.g. CCL1, CXCL8), enzymes (e.g. iNOS, COX-2) and adhesion molecules (e.g. ICAM-1), while the expression of several anti-inflammatory mediators is upregulated (e.g. DUSP1, IκB, IL10, TGFβ, ANXA1, GILZ) [2, 14, 15]. Furthermore, the synthesis of pro-inflammatory agents like prostaglandins, leukotrienes, proteolytic enzymes, free oxygen radicals, and nitric oxide is also inhibited by GCs [14]. Nevertheless, the exact specificity, mechanisms and level of regulation of different inflammatory pathways by the GR signaling have not fully been elucidated. For example, several studies have even revealed immunoenhancing effects of GCs, like the induction of Toll-like Receptor (TLR)2 and TLR4, the secretion of MIF (Macrophage Inhibitory Factor) and the upregulation of IL7Ra which is involved in T cell development [14, 16].

The aim of the present study is to establish a robust *in vivo* model to investigate in detail the molecular mechanism of the anti-inflammatory action of GCs. Profound understanding of the complex interplay of GR with the different components of the immune response may ultimately lead to improved GC treatment regimens, which would be of great importance, since the clinical use of GCs is currently limited by two problems: the deleterious side effects such as skin atrophy, decreased wound healing, osteoporosis, muscle atrophy, glaucoma, psychosis, diabetes mellitus and hypertension [17], and the minority of patients that shows complete or partial resistance to GC treatment [18].

Over the last decade, the zebrafish has emerged in biomedical research as an important model system for a variety of human diseases [19-21]. It is easily handled and maintained and produces big clutches of eggs, which are fertilized externally and develop rapidly [22]. Moreover, its genome has been sequenced and embryos can easily be subjected to genetic manipulations [22, 23]. Additionally, the zebrafish immune system remarkably resembles that of mammals [24], thus providing an excellent research platform for modeling various molecular and cellular elements of inflammation such as host-pathogen interactions during infectious diseases and immune cell migration to wound sites [25, 26]. In the present study, zebrafish larvae are used at three days post fertilization. At this stage, two types of leukocytes are present which constitute the innate immune system, macrophages and neutrophils [27-31]. Cells representing the adaptive immune system, like lymphocytes, start to mature at the second week of zebrafish development [32-34].

Furthermore, the zebrafish is considered as a potent model organism for GC research [35-39]. Zebrafish have a single GR gene which encodes a GR protein that upon activation mediates gene transcription in a similar way as its human equivalent [35, 38, 40, 41]. This zebrafish GR gene also encodes a splice variant, zGRβ, which is the equivalent of the human GR β-isoform [39] that may play a role in resistance to glucocorticoid treatment in humans. As in all teleost fish, cortisol is the main endogenous GC in zebrafish, like in humans, and its secretion is regulated by the hypothalamus pituitary interrenal (HPI) axis, which is the equivalent to the mammalian hypothalamus pituitary adrenal (HPA) axis [36, 37, 42].

Local inflammation can be modeled in zebrafish by amputation of the tail fin of zebrafish larvae [43]. Amputation induces the expression of many pro-inflammatory mediators at the wound site and migration of the two types of leukocytes present at the larval stage, neutrophils and macrophages, towards the site of amputation [41, 43-45]. Interestingly, it has been demonstrated that this migration is inhibited by glucocorticoid treatment and therefore this model system enables studying of the anti-inflammatory action of glucocorticoids in an *in vivo* situation [41, 45].

In the present study we have used the zebrafish tail fin amputation model to study glucocorticoid effects on leukocyte migration and associated changes in gene expression at

the whole transcriptome level. Our results demonstrate that glucocorticoid treatment specifically inhibits the migration of neutrophils and not of macrophages. In addition, we show that tail fin amputation affects the expression of a wide variety of genes, among which many inflammation-related ones, and that glucocorticoid treatment attenuates the vast majority of these changes. Thus, glucocorticoids appear to dampen the inflammatory response in this model system, without any apparent specificity for particular signaling pathways.

Materials & Methods

Zebrafish strains, husbandry & egg collection

Zebrafish were maintained and handled according to the guidelines from the Zebrafish Model Organism Database (ZFIN, http://zfin.org). Fertilization was performed by natural spawning at the beginning of the light period and eggs were raised at 28.5°C in egg water (60μg/ml Instant Ocean sea salts supplemented with 0.0025% methylene blue (GUUR)). All experimental procedures were conducted in compliance with the directives of the local animal welfare committee of Leiden University.

Tail amputation & GC treatment

Three-day-old embryos were anesthetized in egg water containing 0.02% buffered aminobenzoic acid ethyl ester (tricaine, Sigma) and aligned in Petri dishes coated with 2% agarose for subsequent partial amputation of the tail fin as shown in Fig. 1. Amputation was performed using a 1mm sapphire blade (World Precision Instruments) using a Leica M165C stereo-microscope and a micromanipulator. Amputated and non-amputated embryos were pretreated for 2h with either 25μM beclomethasone (Sigma) or vehicle (0.05% DMSO) prior to amputation and again for a specified period of time after amputation (see Results section). For migration studies samples were fixed in 4% paraformaldehyde (PFA) in phosphate-buffered saline (PBS) and stored at 4°C, whereas for gene expression analysis samples were collected in TRIzol® reagent (Invitrogen).

Myeloperoxidase staining and whole mount immunohistochemistry for visualization of macrophages and neutrophils

Embryos were fixed in 4% PFA overnight at 4°C and following washes with PBS containing 0.1% Tween 20 (PBST), the Myeloperoxidase (mpx) activity was detected using the Leukocyte Peroxidase kit (Sigma) according to the manufacturer's instructions. Mpx staining was always performed prior to L-plastin immunohistochemistry. For this purpose, embryos were washed in PBST, gradually dehydrated with methanol in PBS and stored in 100% methanol overnight at 4°C. The next day embryos were rehydrated with graded series of methanol in PBS containing 0.8% Triton X-100 (PBS-TX) and incubated with 10μg/ml Proteinase K (Roche) for 10min at 37°C. Embryos were then incubated in PBS-TX blocking buffer (containing 1% BSA) for 2h at RT and subsequently in blocking buffer containing a rabbit anti-L-plastin polyclonal antibody (provided by Dr. A. Huttenlocher [46], 1:500 dilution) overnight at 4°C. Following washes with PBS-TX, embryos were incubated again in blocking buffer for 1h at RT prior to incubation with goat anti-rabbit Alexa Fluor® 568 dye–labeled secondary antibody (Invitrogen) for 2h at RT (1:200 dilution in blocking buffer).

Imaging of the embryos was performed using a Leica MZ16FA fluorescence stereo-microscope supported by the LAS version 3.7 software. Macrophages were detected based on the red fluorescent labeling by the immunehistochemistry and neutrophils were detected based on their dark brown appearance as a result of the Mpx assay (although they are stained by both methods, the L-plastin immunolabeling is hard to detect in these cells due to the dark staining of the Mpx assay). To determine the number of cells that had migrated to the wounded area, the cells posterior to the caudal vein were counted (marked by the dashed red box in Fig. 1B). Data shown are means (±s.e.m.) of three individual experiments. In each experiment, treatment groups consisted of at least 20 larvae.

RNA isolation & cDNA synthesis

Total RNA was extracted using TRIzol® reagent (Invitrogen) according to the manufacturer's instructions (Invitrogen). RNA was dissolved in water and denatured for 5min at 60°C. Samples were treated with DNAse using the DNA-*free*™ kit (Ambion). For microarray analysis, RNA was further purified using the RNeasy MinElute™ Cleanup kit from Qiagen and its integrity was checked with a lab-on-chip analysis using the 2100 Bioanalyzer (Agilent Technologies). For subsequent cDNA synthesis, 1µg of total RNA was added as a template for reverse transcription using the iSCRIPT™ cDNA Synthesis Kit (Biorad).

Quantitative Polymerase Chain Reaction (qPCR)

QPCR analysis was performed using the MyiQ Single-Color Real-Time PCR Detection System (Biorad). PCR reactions were performed in a total volume of 25µl containing 6.5µl diluted cDNA, 1µl forward and reverse primer (10µM) and 12.5µl of 2x iQ™ SYBR® Green Supermix (Biorad). Cycling conditions were 95°C for 3min, followed by 40 cycles of 15sec at 95°C, 30sec at 60°C and 30sec at 72°C. Ct values (cycle number at which a threshold value of the fluorescence intensity was reached) were determined for each sample. A dissociation protocol was added, determining dissociation of the PCR products from 65°C to 95°C, allowing discrimination of specific products. In all qPCR experiments, a water-control was included. Data shown are means (±s.e.m.) of three individual experiments. In each experiment, cDNA samples were assayed in duplicate. Sequences of all primers used for qPCR analysis are included in Suppl. Table 5.

Microarray design

A 4x180k microarray chip platform (customized by Agilent Technologies, (Design ID:028233)) was used in this study. This array consists of all probes already present in an earlier 45.219 custom-made array [47], and another 126.632 newly designed zebrafish probes had been added as described in [48]. A total of 16 samples (4 experimental groups from 4 replicate experiments) were processed for transcriptome analysis and were hybridized against a common reference.

Microarray amplification & labeling

Amplification and labeling of RNA was performed at the MicroArray Department (MAD) of the University of Amsterdam (Amsterdam, The Netherlands). Per sample, 0.5µg total RNA was amplified and combined with Spike A according to the Agilent Two-Color Microarray-Based Gene Expression Analysis kit (Agilent technologies). As a common reference sample an equimolar pool of all test samples was made and 0.5µg samples were amplified similarly as the test samples with the exception that Spike B was used. Amino-allyl modified nucleotides were incorporated during the aRNA synthesis (2.5mM of each

GTP, ATP, UTP (GE Healthcare), 0.75mM CTP (GE Healthcare), 0.3mM AA-CTP (TriLink Biotechnologies)). Synthesized aRNA was purified with the E.Z.N.A. MicroElute RNA Clean Up Kit (Omega Bio-Tek). The quality was inspected on the BioAnalyzer (Agilent Technologies) with the Agilent RNA 6000 kit (Agilent Technologies). Test samples were labeled with Cy3 and the reference sample was labeled with Cy5. Five µg of aRNA was dried out and dissolved in 50mM carbonate buffer pH 8.5. Individual vials of Cy3/Cy5 from the mono-reactive dye packs (GE Healthcare) were dissolved in 200µl DMSO. To each sample, 10µl of the appropriate CyDye dissolved in DMSO was added and the mixture was incubated for 1h. Reactions were quenched with the addition of 5µl 4M hydroxylamine (Sigma-Aldrich). The labeled aRNA was purified with the E.Z.N.A. MicroElute RNA Clean Up Kit. Yields of aRNA and CyDye incorporation were measured on the NanoDrop ND-1000.

Microarray hybridization, scanning & data processing

Each hybridization mixture was made up from 825ng Test (Cy3-labeled) and 825ng Reference (Cy5-labeled) material. Hybridization mixtures were using the Agilent Two-Color Microarray-Based Gene Expression Analysis kit according to the manufacturer's instructions (Agilent technologies). The samples were loaded onto the microarray chips and hybridized for 17h at 65°C. Afterwards the slides were washed and scanned (20 bit, 3µm resolution) in an ozone-free room with the Agilent G2505C scanner. Data was extracted with Feature Extraction (v10.7.3.1, Agilent Technologies) with the GE2_107_Sep09 protocol for two-color Agilent microarrays. The Agilent output from the 16 hybridizations was then imported into the Rosetta Resolver 7.2 software (Rosetta Biosoftware, Seattle, Washington) and subjected to a factorial design with a re-ratio with common reference application. Data analysis was performed setting cutoff for the p-value of $<10^{-5}$ and for fold change of either >2 or <-2.

Gene Ontology analysis

Gene Ontology analysis was performed with the PathVisio version 2 software (www.pathvisio.org [49]), setting cutoffs for p-value of $<10^{-5}$ and for fold change of either >2 or <-2. For probe annotation, the Ensembl gene ID codes (ENSDARG) were used (see http://www.ensembl.org). The Z-scores shown correspond to a standard statistical test under the hypergeometric distribution. A high Z-score corresponds to a high level of enrichment of genes from a specific pathway in the investigated gene cluster.

Statistical analysis

Statistical analyses (two-way ANOVAs with Bonferroni post-hoc tests) were performed using the GraphPad Prism version 4.00 (GraphPad Software, La Jolla, USA).

Results

The effect of GC treatment on amputation-induced leukocyte migration

Previous studies in zebrafish larvae have shown that leukocytes migrate to wound sites which represents an inflammatory response and that this response is impaired upon treatment with GCs [41, 45]. In order to study this in detail, we set up a tail fin amputation assay using 3 day post fertilization (dpf) larvae that were first exposed to either vehicle or the synthetic GC beclomethasone (25µM) for 2h. Tail fins were then amputated and vehicle or beclomethasone treatment was continued. Samples were collected at 0, 2, 4, 8,

16 and 24h post amputation (hpa) and neutrophils and macrophages were labeled and counted. To determine the number of cells migrated to the wounded area, cells posterior to the caudal vein were counted (area indicated by the dashed red box in Fig. 1B).

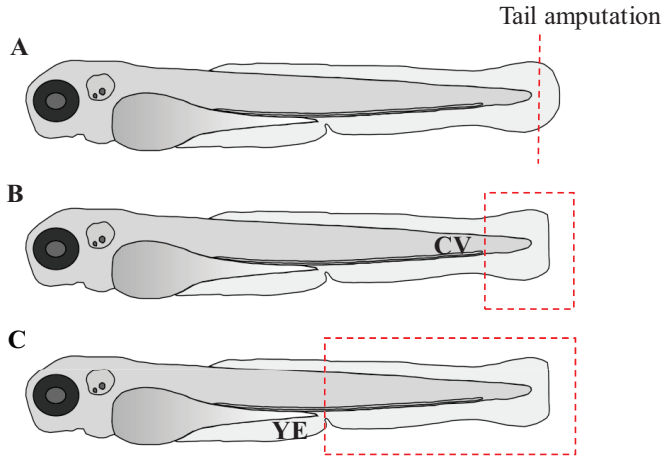

Figure 1. Schematic drawings of a zebrafish larvae at 3dpf (CV = caudal vein, YE = yolk extension). **A**. The site of the tail fin amputation. The red dashed line indicates where the cut in the tail was made. **B**. The area used to determine the number of neutrophils and macrophages that had migrated to the wounded area. The dashed box indicates the area selected for counting. (**C**) The area that is used to determine the total amount of neutrophils and macrophages present in the entire tail region. The dashed box indicates the area selected for counting.

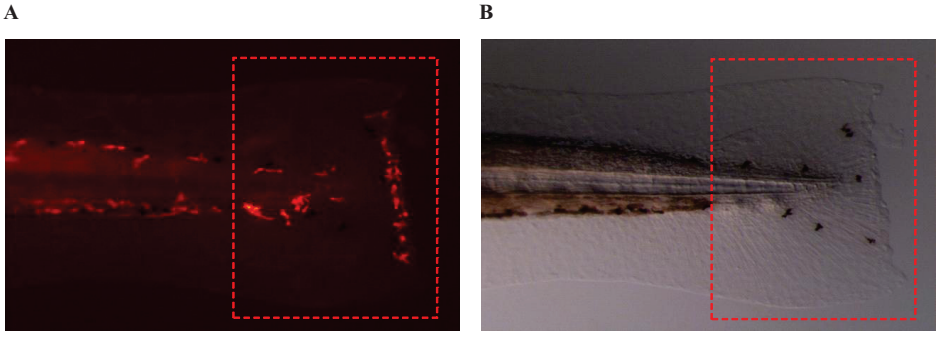

Figure 2. Leukocyte staining upon tail fin amputation in a 3dpf embryo. **A.** Staining of all leukocytes by immunohistochemistry against the pan-leukocyte marker L-plastin (shown in red). **B.** Staining of neutrophils specifically by Mpx staining (shown in black). Neutrophils are stained by both methods, but the L-plastin immunolabeling is hard to detect in these cells due to the dark staining of the Mpx assay. Therefore, the number of neutrophils was determined by counting in the cells stained by the Mpx assay (shown black in A and B) and the number of macrophages was determined by counting the number of cells stained by the L-plastin immunohistochemistry (shown red in A). Cells posterior to the caudal vein were considered to have migrated, so this area (marked by the dashed red box) was used for cell counting.

In order to label the populations of neutrophils and macrophages in 3dpf larvae we employed Myeloperoxidase (Mpx) histochemistry (specifically staining neutrophils [29]), followed by immunolabeling of L-plastin (staining all leukocytes [31]). At this stage of

development two populations of leukocytes are present: neutrophils, which are Mpx- and L-plastin-positive, and macrophages, which are Mpx-negative and L-plastin-positive [27, 29-31, 50]. The number of macrophages was therefore determined by counting the number of cells stained by the L-plastin immunostaining and not stained by the Mpx histochemistry, and the number of neutrophils was determined by counting cells stained by the Mpx assay (although they are stained by both methods, the L-plastin immunolabeling is hard to detect in these cells due to the dark staining of the Mpx assay (Fig. 2)).

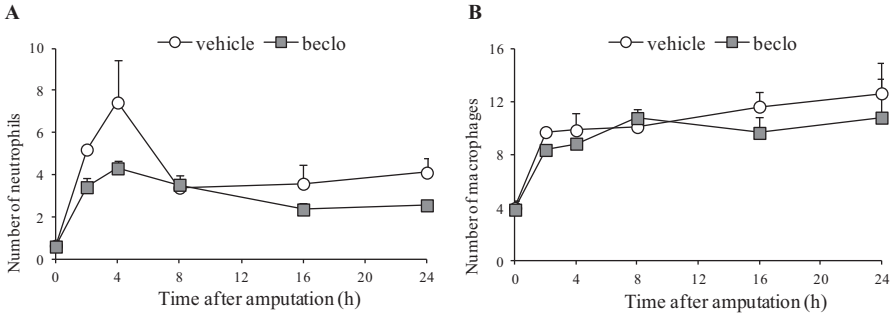

Figure 3. The effect of beclomethasone treatment on leukocyte migration upon tail fin amputation in 3dpf zebrafish larvae. **A.** The number of neutrophils in the wounded area as a function of time after amputation. Statistical analysis by two-way ANOVA revealed that both beclomethasone treatment and time had a significant effect on the number of neutrophils (both $p<0.001$), and that the neutrophil number was significantly increased at 4hpa compared to the 0hpa time point ($p<0.001$). **B.** The number of macrophages in the wounded area as a function of time after amputation. Statistical analysis by two-way ANOVA revealed a migratory response of macrophages over time ($p<0.001$), but that beclomethasone did not have an effect.

The results of this experiment revealed that both neutrophils and macrophages migrate towards the wound site, but that their migratory behavior and response to beclomethasone are remarkably different. Analysis of our data revealed a migratory response of neutrophils over time which was inhibited by beclomethasone treatment (as shown by a significant effect of time and beclomethasone treatment in a two-way ANOVA (both $p<0.001$)). Neutrophil migration reached a peak at 4hpa (7.4 ± 2.0 cells compared to 0.6 ± 0.1 at 0hpa) and rapidly decreased after this time point to 3.4 ± 0.6 at 8hpa after which it remained stable at this level until 24hpa (Fig. 2). Beclomethasone treatment had a significant inhibitory effect on the neutrophil migration at 4hpa (4.3 ± 0.4 cells in the presence of beclomethasone). For macrophages, a migratory response was observed as well ($p<0.001$), but no effect of beclomethasone treatment was observed. Macrophage migration also increased rapidly, especially in the first 2 hours (9.7 ± 0.2 at 2hpa versus 4.0 ± 0.1 0hpa), but no decline was observed afterwards. In addition, macrophages migrated more to the posterior end of the tail where they appeared to line up at the actual wound site, whereas neutrophils were more randomly located in the vicinity of the wound (for representative pictures, see Fig. 2). Based on these results, we concluded that both neutrophils and macrophages migrate towards wound sites, but that beclomethasone exhibits an inhibitory effect only on neutrophil migration.

Subsequently, higher doses of beclomethasone were tested for their inhibitory role on neutrophils and macrophages at 4hpa. These doses did not induce effects on migration different from the 25µM dose that was used in the experiment described above (data not

shown), indicating that at this dose a maximal effect had already been reached. In order to establish that beclomethasone specifically impairs the migration of neutrophils rather than their total number, cells in the entire tail fin area (posterior to the yolk extension) were counted (Fig. 1C). The results of these countings did not show any significant difference in the number of neutrophils between vehicle- and beclomethasone-treated larvae upon amputation (Suppl. Fig. 1), indicating a specific effect of beclomethasone on the neutrophil migration towards wound sites.

Design of the microarray experiment

Next we wanted to investigate the effect of beclomethasone treatment on amputation-induced changes in gene expression at the whole transcriptome level by microarray analysis. For that reason, we employed the tail fin amputation assay described above, collecting total RNA samples at 4hpa. Four experimental groups were generated: control (non-amputated) treated with vehicle (con/vehicle), control treated with beclomethasone (con/beclo), amputated treated with vehicle (4hpa/vehicle) and amputated treated with beclomethasone (4hpa/beclo). Subsequently, the RNA samples from these experimental groups were used in a microarray experiment and the data were analyzed using the Rosetta Resolver 7.2 software, setting signatures for significantly regulated probes at a p-value cutoff of $p < 10^{-5}$ and fold changes either >2 or <-2. Gene annotation and probe assignment was performed based on the Ensemble Gene ID codes (ENSDARG).

The effects of amputation on gene transcription

First, we identified 1403 probes to be significantly regulated due to amputation (comparison con/vehicle vs. 4hpa/vehicle). Gene annotation demonstrated that these probes corresponded to 585 genes, of which 410 were upregulated and 175 downregulated due to amputation. Gene ontology analysis (using PathVisio software) revealed that mainly immune-related signaling routes were affected like the Toll-like, NOD-like and RIG-I-like receptor pathway, the Prostglandin, Cytokine, Interferon, and Jak-STAT signaling pathways as well as Eicosanoid synthesis (Suppl. Table 1).

The effects of beclomethasone treatment on amputation-induced gene transcription

Subsequently, as a first readout of the effect of beclomethasone treatment on amputation-induced changes in gene expression, we studied how amputation-regulated genes generally respond to beclomethasone treatment. Therefore, for each of the 1403 probes that were significantly regulated by amputation we plotted the fold change due to beclomethasone treatment in amputated larvae (comparison 4hpa/vehicle vs. 4hpa/beclomethasone) as a function of the fold change due to amputation (comparison con/vehicle vs. 4hpa/vehicle). In the resulting scatter plot (Fig. 4) probes representing genes that are upregulated by amputation and of which this upregulation is enhanced in the presence of beclomethasone are shown in the upper right quadrant (164 probes representing 69 genes). Probes representing genes that are upregulated by amputation and of which this upregulation is attenuated by beclomethasone are presented in the lower right quadrant (876 probes, 349 genes). Interestingly, this plot demonstrates that the vast majority of probes/genes that are upregulated by amputation shows an attenuation of this upregulation in the presence of beclomethasone. This majority contains 84% of the probes and 83% of the genes showing upregulation by amputation. A similar effect was observed upon studying the probes that showed downregulation by amputation. Of these probes, 92% (363 probes representing 164 genes) displayed an attenuation of this downregulation in the presence of

beclomethasone and is shown in the upper left quadrant, whereas only a small number ended up in the lower left quadrant (32 probes, 14 genes).

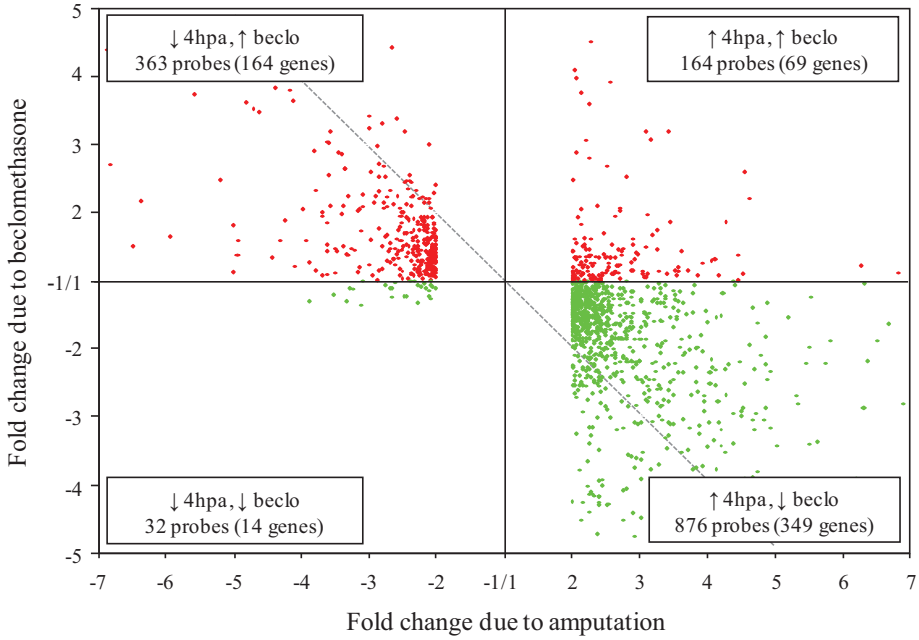

Figure 4. Scatter plot showing the effect of beclomethasone treatment on amputation-induced alterations in gene expression. For all 1403 probes showing significant regulation upon amputation (comparison con/vehicle vs. 4hpa/vehicle), the fold change due to beclomethasone treatment in amputated larvae (4hpa/vehicle vs. 4hpa/beclo) was plotted as a function of the fold change due to amputation. This plot shows that beclomethasone has a very general attenuating effect on amputation-induced gene regulation. Of the 1040 probes showing upregulation by amputation, 84% shows a suppression of this regulation in the presence of beclomethasone (lower right quadrant), and of the 385 probes showing downregulation in response to amputation, 92% shows an attenuated downregulation upon beclomethasone treatment (upper left quadrant). The grey dashed line indicates the point at which beclomethasone treatment completely abolishes amputation-induced changes, showing that in the vast majority of cases beclomethasone dampens the effects of amputation on gene expression, but does not block them entirely.

The grey dashed line in the scatter plot indicates the point at which the regulation by amputation is completely abolished by beclomethasone. Obviously, most of probes in the right lower quadrant are located above this line, indicating that in the majority of cases GC treatment attenuates the amputation-induced gene upregulation, and that it does not completely block it. In the left upper quadrant, a similar effect is shown for the probes downregulated upon amputation. The majority of probes is located below the grey line, indicating that GC treatment does not totally eliminate the amputation-induced downregulation. Taken together, these data show that beclomethasone treatment has a very general attenuating effect on amputation-induced alterations in gene expression, thereby dampening (rather than abolishing) these effects.

Next, we were interested in which individual beclomethasone-induced changes in gene regulation were statistically significant. We first studied the cluster of 410 genes

significantly upregulated by amputation, and found that 94 of these genes (23%) displayed a beclomethasone-induced attenuation of this upregulation that reached significance (Fig. 5A). We subsequently looked at the set of 175 genes downregulated by amputation and 19 genes (11%) showed a beclomethasone-induced attenuation of the downregulation that reached significance (Fig. 5B).

From the cluster of 94 genes that showed a significant upregulation by amputation that was attenuated by beclomethasone, we decided to validate by qPCR the expression of *il8, il1b, mmp9, mmp13a tnfa* and *ptgs2b.* The results demonstrated that 4 of the genes we tested (*il8, il1b, mmp9, mmp13a*) showed a significant induction due to amputation which was then significantly impaired in the presence of beclomethasone (Fig. 6). The other 2 genes (*tnfa* and *ptgs2b*) did not display significant regulation by either amputation or beclomethasone, but a trend showing upregulation due to tail fin injury and GC-mediated attenuation of this effect is present (Fig. 6).

Further gene ontology analysis on this cluster of 94 genes revealed that the majority of the signaling pathways involved were identical to those regulated by amputation (immune-related signaling cascades like the Toll-, RIG-I- and NOD-like receptor, Jak-STAT, and Cytokine signaling and Eicosanoid synthesis pathways (Suppl. Table 2)), indicating that beclomethasone treatment affects virtually all amputation-induced signalimng pathways. Since the Toll-like receptor pathway was represented by a relatively large number of genes (12) in this cluster of 94 genes, we studied the alterations in this pathway in more detail. The results showed that the only Toll-like receptor gene present in this cluster was *tlr5a.* In addition, 3 genes encoded subunits of the AP-1 complex (*fos, junb, atf3*), suggesting an important role for this transcription factor in mediating the attenuation of amputation-induced gene regulation by beclomethasone. Six genes corresponded to cytokines (*il1b, il8, il12a, ifn, tnfa, cxcl-c1c*), and two genes to other pro-inflammatory mediators (*ptgs2b, mmp9)* that are known to be induced upon activation of the Toll-like receptor pathway.

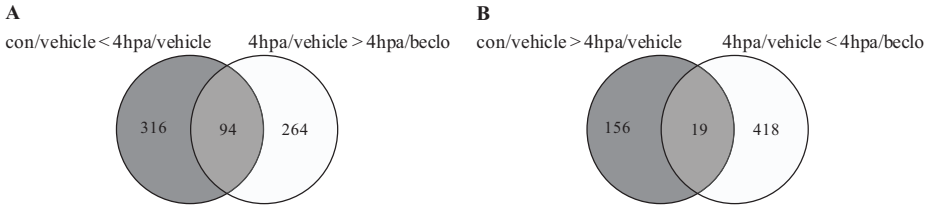

Figure 5. Venn diagrams showing the identification of the cluster of genes significantly regulated by amputation, and showing significant attenuation of this regulation in the presence of beclomethasone. **A**. Genes significantly upregulated due to amputation (410) are shown in the grey circle and genes significantly downregulated by beclomethasone treatment in amputated larvae (358) are shown in the white circle. The overlap represents the cluster of 94 genes of which the amputation-induced upregulation is attenuated by beclomethasone. **B**. Genes significantly downregulated due to amputation (175) are shown in the grey circle and genes significantly upregulated by beclomethasone treatment in amputated larvae (437) are shown in the white circle. The overlap represents the cluster of 19 genes of which the amputation-induced downregulation is attenuated by beclomethasone.

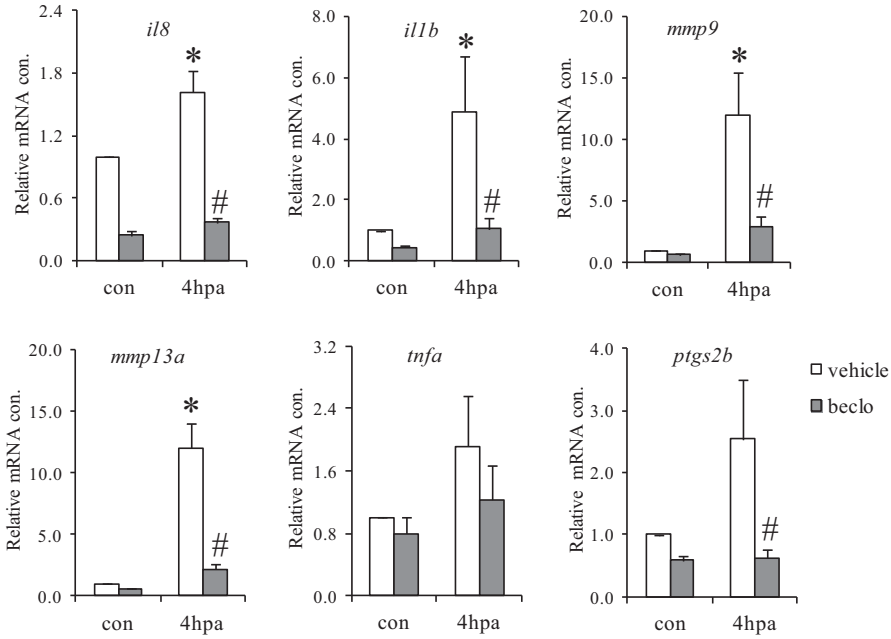

Figure 6. Validation by qPCR of 6 genes (*il8*, *il1b, mmp9*, *mmp13a*, *tnfa* and *ptgs2b)* that showed a significant upregulation by amputation that was attenuated by beclomethasone. The relative mRNA concentrations were normalized to those of *Bactin1* and the values shown are the means ± s.e.m. of four independent experiments. Statistical analysis demonstrated that beclomethasone attenuated the amputation-induced upregualtion of *il8*, *il1b, mmp9* and *mmp13a.* The other genes (*tnfa*, *ptgs2b)* did not reach significance for their induction by amputation (although the trend is present), but in the case of *ptgs2b*, beclomethasone treatment of amputated embryos led to a significant suppression compared to vehicle treated embryos. For *tnfa*, the GC-mediated attenuation did not reach significance. Asterisks (*) correspond to a statistical significance of $p < 0.05$ compared to con/vehicle groups. Key symbols (#) correspond to a statistical significance of $p < 0.05$ compared to 4hpa/vehicle groups.

The effects of beclomethasone on gene transcription

Furthermore, we investigated which genes responded to beclomethasone treatment in non-amputated larvae. A cluster of 2184 probes was identified to be significantly regulated due to beclomethasone treatment (comparison con/vehicle vs con/beclo). Gene annotation demonstrated that these probes corresponded to 815 genes, of which 606 were upregulated and 209 downregulated due to beclomethasone. Gene ontology analysis revealed specific signaling routes to be affected such as those involved in lipid metabolism (e.g. PPAR and adipocytokine signaling and bile acid synthesis pathways) alongside immune-related (e.g. NOD-like receptor and prostaglandin pathways) as well as non-immune related pathways (e.g. DNA replication and sulfur metabolism (Suppl. Table 3)).

Next, we were interested in genes which were significantly changed due to beclomethasone treatment of amputated larvae (comparison 4hpa/vehicle vs. 4hpa/beclo). We identified 2076 probes to be significantly regulated and gene annotation revealed that these probes corresponded to 795 genes, of which 437 were upregulated and 358 were

downregulated. Gene ontology analysis demonstrated that lipid-related cascades (e.g. PPAR signaling and bile acid synthesis pathways) as well as immune-related ones (e.g. Toll-like receptor, prostaglandin signaling and natural killer cell-mediated toxicity pathways) were again affected, alongside phagosome and VEGF signaling pathways (Suppl. Table 4). From these 795 genes, 113 were previously identified to be regulated by amputation and subsequently affected due to beclomethasone treatment (Fig. 5). Additionally, 241 (30%) of these genes were found to be regulated by beclomethasone in non-amputated embryos as well. This latter cluster verifies the validity of our microarray experiment and could provide a reference set of marker genes for studying GR signaling in zebrafish embryos.

Discussion

In the present study, we have used zebrafish larvae in order to study the effects of GC signaling on the inflammatory response to tail fin amputation, both at the cellular and the molecular level. It is well known that upon wounding chemotactic cues attract both neutrophils and macrophages to the wound site in order to combat microbes [51]. In our study, visual detection of macrophages and neutrophils (the former defined as L-plastin-positive and mpx-negative cells, the latter as L-plastin- and mpx-positive [27, 29-31, 50]) revealed that both cell types started to be recruited to the wound site as early as 2hpa. At this time point, macrophage recruitment reached a level which sustained for at least another 22h. Neutrophil migration reached a peak at the 4hpa time point after which their number declined, but remained elevated above basal levels for another 20h (Fig. 3). Previous studies employing similar tissue wounding in zebrafish larvae showed that macrophages [52] and neutrophils [29, 53-55] migrated to the wound sites. In two recent studies [56, 57], the time course of the recruitment of both macrophages and neutrophils to wound sites in the tail fin was studied as well and the results are in line with those from our study. In both studies, neutrophil accumulation at the wounded tissue peaked at around 6hpa, after which numbers declined to baseline, and macrophage migration increased rapidly over the first 6 hours as well and remained at a high level until 48 hpa. In our study, macrophage recruitment appears to be more rapid, reaching a plateau already at 2 hpa, but different ways to define and count the population of macrophages (L-plastin immunohistochemistry in our study versus fms:Gal4/UAS:mCherry transgenic fish [56] and neutral red staining [57]) may underlie the observed differences.

We next examined the effect of GC treatment on the migration of leukocytes towards injured sites. Our analysis showed that beclomethasone treatment had a significant inhibitory effect only on the migration of neutrophils but not on that of macrophages (Fig. 3). These results are in line with previously observed GC effects on leukocytes in 3dpf zebrafish larvae that were shown to be specifically suppressive regarding the recruitment of neutrophils towards wounded tissue but not that of macrophages [45]. Hence, the zebrafish model recapitulates the inhibitory effects of glucocorticoids on neutrophil migration towards inflamed tissues, that have been well established in mammalian models [58]. As for macrophages, studies in mammalian models have shown that GCs can suppress the migratory properties both *in vitro* [59] and *in vivo* [60]. Whether the resistance to GC treatment of macrophages observed in the zebrafish model is specific for fish in general, or the result of the developmental stage of the larvae, the time frame of the assessments, or the selected tissue remains to be investigated.

Subsequently, we evaluated the changes in gene expression that are associated with amputation and beclomethasone treatment. First, we looked for transcriptional changes 4hpa and we identified 585 genes of which the expression was significantly altered upon amputation. These genes are mainly involved in immune-related signaling routes such as that of Toll-like, NOD-like and RIG-I-like receptors, as well as Jak-STAT and cytokine signaling, and Prostaglandin, Interferon, and Eicosanoid synthesis (Suppl. Table 1). Since we used whole larvae for our transcriptional analysis, it must be noted that we do not know in which cell type the induced expression occurs. However, in other studies, it was shown that amputation-induced upregulation of pro-inflammatory genes like *mmp9* and *junb* was mainly observed in the epithelium at the wound site (Mathew 2007, Yoshinari 2009), suggesting that most of the observed amputation-induced alterations in gene expression arise in the tissue around the wound site and not in the immune cells. In a similar study by Yoshinari et al. [61], in which 2dpf embryos were tail fin amputated and samples were collected at a much later time point (16hpa), transcriptome analysis revealed that the largest fraction of regulated signaling routes were metabolic pathways (40%) and only a small fraction (2%) of signaling cascades regulated were immune-related. These results suggest that the time after injury is an important determinant for the alterations in gene transcription that can be observed. Thus, it appears that at 4 hours after injury, immune-related pathways are heavily activated at the transcriptional level, while 12 hours later amputation-induced changes in gene expression no longer reflect an inflammatory response, which is in line with the observed decline in neutrophil migration and the plateau that has been reached in macrophage recruitment at this time point. Most likely, at this stage, the transcriptional response has probably shifted towards the stimulation of regenerative processes.

Second, we were interested in how beclomethasone affected the expression of these amputation-regulated genes. Hence, we plotted for each of the 1403 probes that showed a significant regulation upon amputation the fold change due to beclomethasone treatment in amputated larvae as a function of the fold change due to amputation (Fig. 4). This analysis revealed that the vast majority (83%) of amputation-induced genes showed an attenuated induction in the presence of beclomethasone. Similarly, 94% of the amputation-downregulated genes displayed an attenuation of this downregulation in the presence of beclomethasone (Fig. 4). It must be noted that our data show that in general the transcriptional responses to tail fin injury are not completely blocked by beclomethasone, but that they are dampened. Thus, in this model GCs appear to have a suppressive effect on virtually all changes in gene transcription at 4hpa, which are mainly pro-inflammatory in nature, indicating that GCs have a general immunosuppressive effect without any apparent specificity for particular gene networks.

Ninety-four genes were identified for which both the induction by amputation and the beclomethasone-induced attenuation of this induction reached significance (and 19 genes for which the suppression upon amputation and the attenuation of this suppression by beclomethasone was significant). Gene ontology analysis revealed that within this cluster of 94 genes, immune-related signaling routes were overrepresented, like the Toll-, RIG-I- and NOD-like receptor, Jak-STAT and cytokine signaling and Eicosanoid synthesis pathways. In this gene cluster we found many well-known pro-inflammatory agents, which have been demonstrated to be suppressed upon GC treatment, such as *il8, il1b, tnfa, il11a, il12a, mmp9, mmp13a and ptgs2b* (which is the orthologue of the human *cox-2* gene) [10, 62-66]. For the majority of these genes, it has been well established that DNA-binding-independent transrepression takes place via interaction of GR and immune-related transcription factors, most notably the NF-κB and AP-1 [10, 66]. Thus, the zebrafish

model of wound-induced inflammation recapitulates the anti-inflammatory GC effects with respect to gene transcription observed in mammalian systems, and we therefore suggest that this model system could be further developed as a screening assay for novel GC drugs.

Interestingly, we also found 3 genes encoding AP-1 subunits (*fos, junb, atf3)* in the above mentioned cluster of 94 genes, indicating that, under our experimental conditions, the activity of AP-1 is inhibited by GCs through a decrease in the expression level of several AP-1 subunits. This finding supports an important role for this transcription factor in mediating the attenuation of amputation-induced gene regulation by beclomethasone in zebrafish larvae. A cross-talk (leading to transrepression of pro-inflammatory genes) between GR and AP-1 signaling has been extensively reported to occur via a physical interaction of GR and the c-Jun subunit of AP-1 complex as well as via GR-mediated inhibition of c-Jun activation [67-69]. The downregulation of the expression level observed in our study illustrates that an additional molecular mechanism of negative cross-talk between AP-1 and GR occurs *in vivo*.

Finally, 815 genes were identified that significantly responded to beclomethasone treatment in non-amputated larvae. These genes were attributed to specific signaling routes such as those involved in lipid metabolism (e.g. PPAR and adipocytokine signaling and bile acid synthesis pathways) alongside immune-related (e.g. NOD-like receptor and prostaglandin pathways) as well as non-immune related pathways (e.g. DNA replication and sulfur metabolism (Suppl. Table 3)). Similarly, we identified 795 genes to be significantly changed due to beclomethasone treatment of amputated larvae that gene ontology analysis revealed that lipid-related cascades (e.g. PPAR signaling and bile acid synthesis pathways) as well as immune-related ones (e.g. Toll-like receptor, prostaglandin signaling and natural killer cell-mediated toxicity pathways) were again affected, alongside phagosome and VEGF signaling pathways (Suppl. Table 4). A cluster of 241 genes was found to be regulated by beclomethasone in both amputated and non-amputated larvae. This latter cluster is apparently robustly regulated by GCs, and could therefore provide a reference set of marker genes for studying GR signaling in zebrafish larvae.

In summary, the zebrafish embryonic model of tail fin amputation and GC treatment constitutes a reliable system for studying GR signaling with respect to the innate immune response. In particular, we observed that both macrophages and neutrophils migrated to inflamed tissues and that this course was hindered by GC treatment only in the case of neutrophils. Furthermore, amputation resulted in activation of various immune-related signaling cascades for which GR activation had a general immunosuppressive effect, lacking any apparent specificity for particular signaling cascades. We suggest that this model could in the future be used as a screening assay for novel anti-inflammatory GC drugs.

Acknowledgments

The authors would like to thank Dr. A. Huttenlocher for kindly providing the L-plastin polyclonal antibody. This work was financially supported by the SmartMix program of The Netherlands Ministry of Economic Affairs and the Ministry of Education, Culture and Science.

Supplemental data

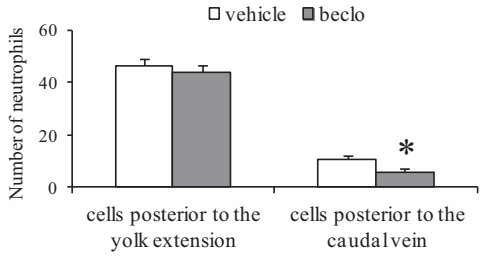

Supplemental Figure 1. Neutrophils present in the entire tail region (posterior to the yolk extension, area marked by the dashed red box in Fig. 1C) compared to neutrophils present in the area close to the wound (posterior to the caudal vein, area marked by the dashed red box in Fig. 1B). Larvae were treated with either vehicle (white bars) or 25μM beclomethasone (grey bars). Statistical analysis showed that beclomethasone does not affect the number of neutrophils present in the entire tail region, but only the number of cells localized in the area close to the wound. The asterisk (*) corresponds to a statistically significant difference in area close to the wound compared to vehicle treatment ($p<0.05$).

Pathway	Genes meeting criteria	Z score
Response to infection *	39	10.31
Toll-like receptor pathway	22	7.05
Prostaglandin signaling	7	4.86
Cytokine-cytokine receptor interaction	12	3.41
Jak-STAT signaling pathway	10	3.27
Eicosanoid Synthesis	3	3.2
NOD-like receptor signaling pathway	6	3.18
RIG-I-like receptor signaling pathway	6	2.92
Pantothenate and CoA biosynthesis	2	2.68
IFN Pathway	10	2.34

Supplemental Table 1: Pathways enriched in cluster of 585 genes regulated upon amputation, determined by gene ontology analysis using PathVisio software (p-value cutoff $<10^{-5}$, fold change >2 or <-2). * Reference set based on *Mycobacterium marinum* yolk infection.

Pathway	Genes meeting criteria	Z score
Response to infection *	16	9.07
Toll-like receptor pathway	12	8.78
Eicosanoid Synthesis	2	4.73
Cytokine-cytokine receptor interaction	6	4.33
RIG-I-like receptor signaling pathway	4	3.72
NOD-like receptor signaling pathway	3	3.71
Arachidonic acid metabolism	2	3.15
Cytosolic DNA-sensing pathway	2	3.15
Jak-STAT signaling pathway	4	3.06
Pantothenate and CoA biosynthesis	1	2.88

Supplemental Table 2: Pathways enriched in cluster of 94 genes that showed an upregualtion by amputation, which was attenuated by beclomethasone, determined by gene ontology analysis using PathVisio software (p-value cutoff $<10^{-5}$, fold change >2 or <-2). * Reference set based on *Mycobacterium marinum* yolk infection.

Pathway	Genes meeting criteria	Z score
Primary bile acid biosynthesis	4	5.11
NOD-like receptor signaling pathway	8	4.49
PPAR signaling pathway	9	4.35
Prostaglandin signaling	6	3.81
Response to infection*	21	3.8
Nuclear receptors in lipid metabolism and toxicity	4	3.36
NOD pathway	7	3.14
Sulfur metabolism	2	3.08
DNA Replication	4	2.35
Adipocytokine signaling pathway	6	2.12

Supplemental Table 3: Pathways enriched in gene cluster (815 genes) regulated by beclomethasone, determined by gene ontology analysis using PathVisio software (p-value cutoff $<10^{-5}$, fold change >2 or <-2). * Reference set based on *Mycobacterium marinum* yolk infection.

Pathway	Genes meeting criteria	Z score
PPAR signaling pathway	12	5.25
Toll-like receptor pathway	21	4.98
Prostaglandin signaling	8	4.59
Natural killer cell-mediated cytotoxicity	12	4.03
Response to infection*	23	3.18
Primary bile acid biosynthesis	3	3.08
NOD pathway	8	3.01
Taurine and hypotaurine metabolism	2	2.91
Phagosome	14	2.64
VEGF signaling pathway	9	2.64

Supplemental Table 4: Pathways enriched in gene cluster (795 genes) regulated by beclomethasone in amputated larvae, determined by gene ontology analysis using PathVisio software (p-value cutoff $<10^{-5}$, fold change >2 or <-2). * Reference set based on *Mycobacterium marinum* yolk infection.

Gene name	Gene symbol	Forward primer sequence	Reverse primer sequence
Bactin1	*Bactin1*	CGAGCAGGAGATGGGAACC	CAACGGAAACGCTCATTGC
interleukin 8	*il8*	TGTGTTATTGTTTTCCTGGCATTTC	GCGACAGCGTGGATCTACAG
interleukin 1, beta	*Il1b*	CATAAACACCTTCGAGTCcG	TCTTTCCTGTCCATCTCCACCA
matrix metalloproteinase 9	*mmp9*	CATTAAAGATGCCCTGATGTATCCC	AGTGGTGGTCCGTGGTTGAG
matrix metalloproteinase 13a	*mmp13a*	ATGGTGCAAGGCTATCCCAAGAGT	GCCTGTTGTTGGAGCCAAACTCAA
tumor necrosis factor a	*tnfa*	AGACCTTAGACTGGAGAGATGAC	CAAAGACACCTGGCTGTAGAC
prostaglandin-endoperoxide synthase 2b	*ptgs2b*	TGGGCTTCGTGGTTTGCACAGG	GCGTCGGAGCCCATTTCCGT

Supplemental Table 5: Sequences of all primers used for qPCR analysis.

References

1. Franchimont, D., et al., *Glucocorticoids and inflammation revisited: the state of the art. NIH clinical staff conference.* Neuroimmunomodulation, 2002. **10**(5): p. 247-60.
2. Coutinho, A.E. and K.E. Chapman, *The anti-inflammatory and immunosuppressive effects of glucocorticoids, recent developments and mechanistic insights.* Mol Cell Endocrinol, 2011. **335**(1): p. 2-13.
3. Heitzer, M.D., et al., *Glucocorticoid receptor physiology.* Rev Endocr Metab Disord, 2007. **8**(4): p. 321-30.
4. Schoneveld, O.J., I.C. Gaemers, and W.H. Lamers, *Mechanisms of glucocorticoid signalling.* Biochim Biophys Acta, 2004. **1680**(2): p. 114-28.
5. Sapolsky, R.M., L.M. Romero, and A.U. Munck, *How do glucocorticoids influence stress responses? Integrating permissive, suppressive, stimulatory, and preparative actions.* Endocr Rev, 2000. **21**(1): p. 55-89.
6. Revollo, J.R. and J.A. Cidlowski, *Mechanisms generating diversity in glucocorticoid receptor signaling.* Ann N Y Acad Sci, 2009. **1179**: p. 167-78.
7. de Kloet, E.R., M. Joels, and F. Holsboer, *Stress and the brain: from adaptation to disease.* Nat Rev Neurosci, 2005. **6**(6): p. 463-75.
8. Chrousos, G.P. and T. Kino, *Intracellular glucocorticoid signaling: a formerly simple system turns stochastic.* Sci STKE, 2005. **2005**(304): p. pe48.
9. Nicolaides, N.C., et al., *The human glucocorticoid receptor: molecular basis of biologic function.* Steroids, 2010. **75**(1): p. 1-12.
10. De Bosscher, K. and G. Haegeman, *Minireview: latest perspectives on antiinflammatory actions of glucocorticoids.* Mol Endocrinol, 2009. **23**(3): p. 281-91.
11. van der Laan, S. and O.C. Meijer, *Pharmacology of glucocorticoids: beyond receptors.* Eur J Pharmacol, 2008. **585**(2-3): p. 483-91.
12. Buckingham, J.C., *Glucocorticoids: exemplars of multi-tasking.* Br J Pharmacol, 2006. **147 Suppl 1**: p. S258-68.
13. Beato, M. and J. Klug, *Steroid hormone receptors: an update.* Hum Reprod Update, 2000. **6**(3): p. 225-36.
14. Franchimont, D., *Overview of the actions of glucocorticoids on the immune response: a good model to characterize new pathways of immunosuppression for new treatment strategies.* Ann N Y Acad Sci, 2004. **1024**: p. 124-37.
15. Barnes, P.J., *Glucocorticosteroids: current and future directions.* Br J Pharmacol, 2011. **163**(1): p. 29-43.
16. Galon, J., et al., *Gene profiling reveals unknown enhancing and suppressive actions of glucocorticoids on immune cells.* FASEB J, 2002. **16**(1): p. 61-71.

17. Schacke, H., W.D. Docke, and K. Asadullah, *Mechanisms involved in the side effects of glucocorticoids.* Pharmacol Ther, 2002. **96**(1): p. 23-43.
18. Barnes, P.J. and I.M. Adcock, *Glucocorticoid resistance in inflammatory diseases.* Lancet, 2009. **373**(9678): p. 1905-17.
19. Brittijn, S.A., et al., *Zebrafish development and regeneration: new tools for biomedical research.* Int J Dev Biol, 2009. **53**(5-6): p. 835-50.
20. Xi, Y., S. Noble, and M. Ekker, *Modeling neurodegeneration in zebrafish.* Curr Neurol Neurosci Rep, 2011. **11**(3): p. 274-82.
21. Lieschke, G.J. and P.D. Currie, *Animal models of human disease: zebrafish swim into view.* Nat Rev Genet, 2007. **8**(5): p. 353-67.
22. Kari, G., U. Rodeck, and A.P. Dicker, *Zebrafish: an emerging model system for human disease and drug discovery.* Clin Pharmacol Ther, 2007. **82**(1): p. 70-80.
23. Kawakami, K., *Transposon tools and methods in zebrafish.* Dev Dyn, 2005. **234**(2): p. 244-54.
24. Trede, N.S., et al., *The use of zebrafish to understand immunity.* Immunity, 2004. **20**(4): p. 367-79.
25. Meijer, A.H. and H.P. Spaink, *Host-pathogen interactions made transparent with the zebrafish model.* Curr Drug Targets, 2011. **12**(7): p. 1000-17.
26. Meeker, N.D. and N.S. Trede, *Immunology and zebrafish: spawning new models of human disease.* Dev Comp Immunol, 2008. **32**(7): p. 745-57.
27. Herbomel, P., B. Thisse, and C. Thisse, *Ontogeny and behaviour of early macrophages in the zebrafish embryo.* Development, 1999. **126**(17): p. 3735-45.
28. Bennett, C.M., et al., *Myelopoiesis in the zebrafish, Danio rerio.* Blood, 2001. **98**(3): p. 643-51.
29. Lieschke, G.J., et al., *Morphologic and functional characterization of granulocytes and macrophages in embryonic and adult zebrafish.* Blood, 2001. **98**(10): p. 3087-96.
30. Crowhurst, M.O., J.E. Layton, and G.J. Lieschke, *Developmental biology of zebrafish myeloid cells.* Int J Dev Biol, 2002. **46**(4): p. 483-92.
31. Meijer, A.H., et al., *Identification and real-time imaging of a myc-expressing neutrophil population involved in inflammation and mycobacterial granuloma formation in zebrafish.* Dev Comp Immunol, 2008. **32**(1): p. 36-49.
32. Willett, C.E., et al., *Early hematopoiesis and developing lymphoid organs in the zebrafish.* Dev Dyn, 1999. **214**(4): p. 323-36.
33. Davidson, A.J. and L.I. Zon, *The 'definitive' (and 'primitive') guide to zebrafish hematopoiesis.* Oncogene, 2004. **23**(43): p. 7233-46.
34. Lam, S.H., et al., *Development and maturation of the immune system in zebrafish, Danio rerio: a gene expression profiling, in situ hybridization and immunological study.* Dev Comp Immunol, 2004. **28**(1): p. 9-28.
35. Schaaf, M.J., A. Chatzopoulou, and H.P. Spaink, *The zebrafish as a model system for glucocorticoid receptor research.* Comp Biochem Physiol A Mol Integr Physiol, 2009. **153**(1): p. 75-82.
36. Alsop, D. and M.M. Vijayan, *Molecular programming of the corticosteroid stress axis during zebrafish development.* Comp Biochem Physiol A Mol Integr Physiol, 2009. **153**(1): p. 49-54.
37. Steenbergen, P.J., M.K. Richardson, and D.L. Champagne, *The use of the zebrafish model in stress research.* Prog Neuropsychopharmacol Biol Psychiatry, 2011. **35**(6): p. 1432-51.
38. Schoonheim, P.J., A. Chatzopoulou, and M.J. Schaaf, *The zebrafish as an in vivo model system for glucocorticoid resistance.* Steroids, 2010. **75**(12): p. 918-25.
39. Schaaf, M.J.M., et al., *Discovery of a Functional Glucocorticoid Receptor β -Isoform in Zebrafish.* Endocrinology, 2008. **149**(4): p. 1591-1599.
40. Hillegass, J.M., et al., *Glucocorticoids alter craniofacial development and increase expression and activity of matrix metalloproteinases in developing zebrafish (Danio rerio).* Toxicol Sci, 2008. **102**(2): p. 413-24.
41. Zhang, Y., et al., *In vivo interstitial migration of primitive macrophages mediated by JNK-matrix metalloproteinase 13 signaling in response to acute injury.* J Immunol, 2008. **181**(3): p. 2155-64.
42. Wendelaar Bonga, S.E., *The stress response in fish.* Physiol Rev, 1997. **77**(3): p. 591-625.
43. Renshaw, S.A., et al., *A transgenic zebrafish model of neutrophilic inflammation.* Blood, 2006. **108**(13): p. 3976-8.
44. Ellett, F., et al., *mpeg1 promoter transgenes direct macrophage-lineage expression in zebrafish.* Blood, 2011. **117**(4): p. e49-56.
45. Mathew, L.K., et al., *Unraveling tissue regeneration pathways using chemical genetics.* J Biol Chem, 2007. **282**(48): p. 35202-10.
46. Mathias, J.R., et al., *Live imaging of chronic inflammation caused by mutation of zebrafish Hai1.* J Cell Sci, 2007. **120**(Pt 19): p. 3372-83.

47. Stockhammer, O.W., et al., *Transcriptome analysis of Traf6 function in the innate immune response of zebrafish embryos.* Mol Immunol, 2010. **48**(1-3): p. 179-90.
48. Rauwerda, H., et al., *Integrating heterogeneous sequence information for transcriptome-wide microarray design; a Zebrafish example.* BMC Res Notes, 2010. **3**: p. 192.
49. van Iersel, M.P., et al., *Presenting and exploring biological pathways with PathVisio.* BMC Bioinformatics, 2008. **9**: p. 399.
50. Le Guyader, D., et al., *Origins and unconventional behavior of neutrophils in developing zebrafish.* Blood, 2008. **111**(1): p. 132-41.
51. Martin, P. and S.J. Leibovich, *Inflammatory cells during wound repair: the good, the bad and the ugly.* Trends Cell Biol, 2005. **15**(11): p. 599-607.
52. Mathias, J.R., et al., *Characterization of zebrafish larval inflammatory macrophages.* Dev Comp Immunol, 2009. **33**(11): p. 1212-7.
53. Mathias, J.R., et al., *Resolution of inflammation by retrograde chemotaxis of neutrophils in transgenic zebrafish.* J Leukoc Biol, 2006. **80**(6): p. 1281-8.
54. Niethammer, P., et al., *A tissue-scale gradient of hydrogen peroxide mediates rapid wound detection in zebrafish.* Nature, 2009. **459**(7249): p. 996-9.
55. Renshaw, S.A., et al., *Modeling inflammation in the zebrafish: how a fish can help us understand lung disease.* Exp Lung Res, 2007. **33**(10): p. 549-54.
56. Gray, C., et al., *Simultaneous intravital imaging of macrophage and neutrophil behaviour during inflammation using a novel transgenic zebrafish.* Thromb Haemost, 2011. **105**(5): p. 811-9.
57. Loynes, C.A., et al., *Pivotal Advance: Pharmacological manipulation of inflammation resolution during spontaneously resolving tissue neutrophilia in the zebrafish.* J Leukoc Biol, 2010. **87**(2): p. 203-12.
58. Pitzalis, C., N. Pipitone, and M. Perretti, *Regulation of leukocyte-endothelial interactions by glucocorticoids.* Ann N Y Acad Sci, 2002. **966**: p. 108-18.
59. Patsouris, D., et al., *Glucocorticoids and thiazolidinediones interfere with adipocyte-mediated macrophage chemotaxis and recruitment.* J Biol Chem, 2009. **284**(45): p. 31223-35.
60. Zhang, D., et al., *Restraint stress-induced immunosuppression by inhibiting leukocyte migration and Th1 cytokine expression during the intraperitoneal infection of Listeria monocytogenes.* J Neuroimmunol, 1998. **92**(1-2): p. 139-51.
61. Yoshinari, N., et al., *Gene expression and functional analysis of zebrafish larval fin fold regeneration.* Dev Biol, 2009. **325**(1): p. 71-81.
62. Rae, M.T., et al., *Glucocorticoid receptor-mediated regulation of MMP9 gene expression in human ovarian surface epithelial cells.* Fertil Steril, 2009. **92**(2): p. 703-8.
63. Bamberger, C.M., et al., *Vitamin B6 modulates glucocorticoid-dependent gene transcription in a promoter- and cell type-specific manner.* Exp Clin Endocrinol Diabetes, 2004. **112**(10): p. 595-600.
64. Richardson, D.W. and G.R. Dodge, *Dose-dependent effects of corticosteroids on the expression of matrix-related genes in normal and cytokine-treated articular chondrocytes.* Inflamm Res, 2003. **52**(1): p. 39-49.
65. Tuckermann, J.P., et al., *The DNA binding-independent function of the glucocorticoid receptor mediates repression of AP-1-dependent genes in skin.* J Cell Biol, 1999. **147**(7): p. 1365-70.
66. Barnes, P.J., *Corticosteroid effects on cell signalling.* Eur Respir J, 2006. **27**(2): p. 413-26.
67. De Bosscher, K., W. Vanden Berghe, and G. Haegeman, *The interplay between the glucocorticoid receptor and nuclear factor-kappaB or activator protein-1: molecular mechanisms for gene repression.* Endocr Rev, 2003. **24**(4): p. 488-522.
68. Necela, B.M. and J.A. Cidlowski, *Mechanisms of glucocorticoid receptor action in noninflammatory and inflammatory cells.* Proc Am Thorac Soc, 2004. **1**(3): p. 239-46.
69. Newton, R. and N.S. Holden, *Separating transrepression and transactivation: a distressing divorce for the glucocorticoid receptor?* Mol Pharmacol, 2007. **72**(4): p. 799-809.